Available online at www.sciencedirect.com
SCIENCE DIRECT®
Journal of Sound and Vibration 282 (2005) 37–60
JOURNAL OF SOUND AND VIBRATION
www.elsevier.com/locate/jsvi

Dynamic force identification based on enhanced least squares and total least-squares schemes in the frequency domain

Yi Liu, W. Steve Shepard Jr.*

The University of Alabama, Department of Mechanical Engineering, Tuscaloosa, AL 35487, USA

Received 18 August 2003; accepted 14 February 2004
Available online 22 September 2004

Abstract

Identifying dynamic forces from structural responses is necessary when direct measurement of those dynamic forces is impossible using conventional means. A common approach to address this problem is to determine the frequency response function (FRF) matrix, measure the structural responses, and calculate the dynamic forces based on least-squares (LS) scheme. This approach has been proven to be effective in reducing the random errors that occur in structural response signals. Unfortunately, the accuracy of this approach is often hindered by the inversion of an ill-conditioned FRF matrix at frequencies near the structural resonances. To overcome this inversion instability, two regularization filters, namely the truncated singular value decomposition (TSVD) filter and the Tikhonov filter, are used in conjunction with the conventional LS scheme at specific frequencies. Here a criterion for applying these enhanced LS schemes is proposed to aid in determining when the increase in computational effort is better utilized. Furthermore, a new LS form of the Morozov's discrepancy principle is formulated to aid in selecting the optimum regularization parameter for these filters at each frequency. The accuracy in using conventional LS, TSVD-based LS, and Tikhonov filter-based LS schemes are compared analytically and numerically in this paper. It is found that for small-sized FRF matrices, the Tikhonov filter-based LS scheme tends to work better than the TSVD filter-based LS scheme. Since these approaches can only deal with the random errors in the measured structural responses, a total least-squares (TLS) scheme that can also address errors associated with the FRF matrix is proposed in this research. Numerical simulations demonstrate that under certain conditions, the TLS scheme is more effective in reducing the impact of these errors.

*Corresponding author. Tel: +1-205-348-0048; fax: +1-205-348-6419.
E-mail address: sshepard@coe.eng.ua.edu (W.S. Shepard Jr.).

0022-460X/$ - see front matter © 2004 Elsevier Ltd. All rights reserved.
doi:10.1016/j.jsv.2004.02.041

Nomenclature

y	structural response
x	coordinate specifying a point of the structure
x_0	coordinate specifying a point of the structure
t	time
τ	dummy variable
$\mathbf{A}$	FRF matrix
ω	angular velocity
f	exciting force
m	number of measurement locations
n	number of identified forces
η	error
$\mathbf{U}$	left unitary matrix of singular-value decomposition
$\mathbf{V}$	right unitary matrix of singular-value decomposition
$\mathbf{\Sigma}$	singular-value matrix
s	singular value
W_α	filter function
ε	error norm
κ	2-norm condition number
$\Delta\mathbf{A}$	perturbation matrix
$\Delta\mathbf{y}$	perturbation response
k	regularization parameter for truncated TLS scheme
α	regularization parameter for LS scheme
f_{tls}	TLS solution
F_1	dynamic force one
F_2	dynamic force two
Δy_i	amplitude Gaussian noise
$\Delta\varphi$	phase Gaussian noise
ξ_t	discrepancy

Superscripts

H	Hermitian transpose
$+$	pseudo-inverse
-1	inverse
t	time
noisy	noise
identified	identified value
exact	exact value

Subscripts

pol	polluted value
exact	exact value
α	regularization parameter

1. Introduction

Accurate identification of dynamic forces can be very important to the structural design process. Unfortunately, in some cases it is impossible to insert force gauges into the force transfer path to measure those dynamic forces directly. Therefore, indirectly inferring these dynamic forces by using measured structural motion responses in some sort of inverse model is sometimes necessary. Among the conventional force identification methods, the frequency response function (FRF)-based least-squares approach [1] is the most widely used because it can be applied to a variety of force identification problems. The basic premise of the FRF approach is based on spectral analysis. Given the measured vibrational response at one or more locations and the frequency-domain FRF matrix, one can back-calculate the dynamic excitation forces at each specific frequency by pre-multiplying the measured response vector by the pseudo-inverse of the FRF matrix at that frequency. The pseudo-inverse technique is also known as a least-squares method. An inverse Fourier transform on these computed values provides a time history of the dynamic forces, which is of great interest in many cases such as impact force identification. Note that depending on the number of measured response points and other important parameters, this technique can be used to find a single force or a set of forces acting on the structure.

The least-squares approach does have important limitations, however. Some of the applications and limitations of this approach are discussed next. Then existing methods for overcoming some of these limitations are reviewed.

In, 1979, Bartlett [2] applied the least-square scheme to determine vibratory vertical and lateral hub forces in an experimental helicopter model. Fourteen accelerometers were installed on a 5-foot-long helicopter to indirectly determine these forces. The reasonableness of the forces identified in that effort testifies to the success of the method. N. Okubo also successfully identified dynamic forces by applying this approach on various structures [3]. Unfortunately, in spite of some successful applications, the accuracy of this approach can still be hindered by the direct inversion of an ill-conditioned FRF matrix at frequencies near the structural resonances. Fabunmi [4,5] provided some insight on the causes of the inversion difficulties near resonant frequencies by investigating the structural modes participating in the FRF matrix. He found that at a given frequency the number of orthogonal modes, both rigid and elastic, that participate significantly in the FRF matrix has a direct relationship with the condition of the FRF matrix. Because only one mode dominates the FRF matrix near resonances for a lightly damped structure, the FRF matrix tends to be ill-conditioned and the LS scheme is most likely to fail at these frequencies. The pseudo-inverse of an ill-conditioned matrix can be numerically unsolvable or numerically unstable with regard to error in the responses [6]. Although this ill-conditioning can be a major problem, there are techniques that have been developed for addressing this issue. If the inversion is numerically unstable, one is still able to achieve computational stability by introducing regularization filters into the LS scheme. These filters, which are described using a regularization parameter, increase inverse stability by adding constraints to the solution [7]. Two of these approaches will be described next in more detail.

In the area of mathematics, the truncated singular value decomposition (TSVD) and the Tikhonov filter have been developed to increase inverse stability. In effect, the TSVD technique can be described as a filter that helps overcome the instability by filtering out the smallest singular values of the matrix. In contrast, the Tikhonov filter tends to improve the inverse instability by modifying the singular values through a regularization parameter [7]. In a recent study, Thite [8,9] used different methods to increase inverse stability for a transfer path analysis problem. Through numerical studies, he found that the Tikhonov filter works better than the TSVD filter in identifying coherent dynamic forces. However, no explanation was given why the Tikhonov filter is superior to the TSVD filter. Additionally, no specific criterion for applying these filters-based LS schemes is suggested, hence making it quite inefficient to apply these complicated filters at each specific frequency. It is worth noting that in Thite's work, the FRF matrix used in both the numerical and experimental studies was polluted. The analytical matrix was polluted by modal truncation errors while the experimental matrix was polluted with measurement errors. However, if these errors are negligible compared with the exact FRF matrix or the errors in structural responses are dominant, the computed FRF matrix can be assumed as 'exact' and the TSVD and Tikhonov filter provides improved results in these cases [8]. It is also known that the FRF matrix is likely to be polluted by relatively large modeling or measurement errors when the structure is not well quantified. These errors tend to result in large inversion errors near resonances [5]. Unfortunately, no satisfactory algorithm has been proposed to deal with this problem.

A major focus of the work presented here is to provide an effective and efficient algorithm for force identification problems. First, a criterion of applying these enhanced LS schemes, namely

the TSVD and the Tikhonov filter-based LS schemes, is developed. Then the Tikhonov filter is reformulated in a form that tends to give a clear comparison with the TSVD filter approach. It has been shown that the discrepancy principle has a more desirable convergence rate than any other parameter choice law used in previous studies [7–9]. Hence, in order to achieve a better regularization result, a new LS form of Morozov's discrepancy principle is developed in this work to determine the optimum regularization parameters. Theoretical and numerical studies are used to show that the Tikhonov filter can achieve better results than the TSVD filter when the size of FRF matrix is small. Another objective of this paper is to examine the possibility of applying a total least square (TLS) scheme to reduce the measurement errors in both the FRF matrix and the structural responses. The numerical study reveals that under certain conditions, the TLS scheme is more effective than the LS scheme.

The following section provides an overview of the conventional LS scheme for force identification problems. Although details associated with this dynamic force identification method can be found in another work [10], a brief overview of the technique is provided here for completeness. Along with this discussion, some of the limitations of this technique are again noted and the methods mentioned above for overcoming these limitations are discussed in more detail.

2. Force identification based on Least-square scheme

The translational response $y(x,t)$ at a discrete point x on a structure is related to the input or excitation force $f(x_0,t)$, located at x_0, by the Green's function $A(x|x_0,t)$ in integral form as [1]

$$y(x,t) = \int_0^t A(x|x_0, t-\tau) f(x_0, \tau)\, \mathrm{d}\tau. \tag{1}$$

Applying the Fourier transform to both sides of Eq. (1) and rearranging, the deconvolution formulation in the frequency domain is obtained as

$$\tilde{y}(x,\omega) = \tilde{A}(x|x_0,\omega) \cdot \tilde{f}(x_0, \omega), \tag{2}$$

where $\tilde{f}$, $\tilde{y}$, and $\tilde{A}$ are complex functions of the harmonic frequency ω.

In general, Eq. (2) can be expressed in matrix form if multiple responses are measured at different locations using the relationship

$$\tilde{\mathbf{y}}(\omega)_{m\times 1} = \tilde{\mathbf{A}}(\omega)_{m\times n} \cdot \tilde{\mathbf{f}}(\omega)_{n\times 1}, \tag{3}$$

where m refers to the number of the measurement locations, and n is the number of forces to be identified. $\tilde{\mathbf{A}}(\omega)$ is the FRF matrix with $\tilde{A}_{ij}(\omega)$ being the frequency response function between the measured response at x_i and the force located at location x_j. If $\tilde{\mathbf{y}}(\omega)$ and $\tilde{\mathbf{A}}(\omega)$ are known and $m=n$, Eq. (3) can be pre-multiplied by $\tilde{\mathbf{A}}^{-1}(\omega)$ to indirectly compute the desired force $\tilde{\mathbf{f}}(\omega)$.

To reduce the impact of any errors in the measured response signals, it is generally better to use a least-squares (LS) scheme with $m>n$ when back-calculating the input forces. The LS scheme provides some redundancy by utilizing response measurements taken at extra locations in order to reduce the measured error and thereby improve the accuracy of the identified forces. The resulting

formulation is

$$\tilde{\mathbf{f}} = \tilde{\mathbf{A}}^{+}\tilde{\mathbf{y}}, \tag{4}$$

where the shortened notations $\tilde{\mathbf{f}} = \tilde{\mathbf{f}}(\omega)$, $\tilde{\mathbf{A}} = \tilde{\mathbf{A}}(\omega)$, and $\tilde{\mathbf{y}} = \tilde{\mathbf{y}}(\omega)$ are adopted for simplicity. $\tilde{\mathbf{A}}^{+}$ refers to the pseudo-inverse of the non-square matrix $\tilde{\mathbf{A}}$, which is defined by [1]

$$\tilde{\mathbf{A}}^{+} = (\tilde{\mathbf{A}}^{H}\tilde{\mathbf{A}})^{-1}\tilde{\mathbf{A}}^{H}, \tag{5}$$

where the superscript H refers to the Hermitian transpose.

Once the measured structural responses and the FRF matrix are obtained, the dynamic forces can be computed from Eq. (4). However, the success of this formulation largely depends upon the accuracy of the matrix inversion process. If the matrix $\tilde{\mathbf{A}}$ is ill-conditioned, the error in the structural responses $\tilde{\mathbf{y}}$ will actually be amplified and the overall accuracy of the identified forces will be reduced dramatically. In some cases, this ill-conditioning yields a relationship that is unsolvable [6].

One possible way to address this error amplification problem in the LS scheme is to implement a regularization method. This regularization can be accomplished if a numerical solution to Eq. (3) exists. The idea of a TSVD filter to provide such a regularization has been employed in the force identification technique for a long time [11]. However, this filter is not an ideal solution for force identification problems since a lot of useful dynamic information tends to be filtered out by the TSVD method. In contrast, another regularization method, the Tikhonov filter, is able to retain more dynamic information than the TSVD filter especially when the size of FRF matrix is small. This difference has not been explicitly stated in any previous literature and hence it is difficult to select an optimum filter for each application. In the following section, the Tikhonov filter is given in an alternative form that tends to provide a more in-depth understanding of the differences between the TSVD filter and the Tikhonov filter methods. In addition, since the inverse singularity issues described above do not occur at each frequency, a criterion for applying these enhanced LS schemes is proposed. The suggestion of such a criterion has not been addressed before now.

3. TSVD, Tikhonov filter-based LS schemes, and application criterion

Consider some vector $\tilde{\boldsymbol{\eta}}$ that describes the error in the measurement of the structural responses

$$\tilde{\mathbf{y}}_{\text{pol}} = \tilde{\mathbf{A}}\tilde{\mathbf{f}}_{\text{exact}} + \tilde{\boldsymbol{\eta}}, \tag{6}$$

where $\tilde{\mathbf{f}}_{\text{exact}}$ refers to exact dynamic forces (i.e. the actual excitation force), and $\tilde{\mathbf{y}}_{\text{pol}}$ is the polluted responses containing that error. Note here that the FRF matrix $\tilde{\mathbf{A}}$ is assumed to be polluted by negligible modeling or measurement errors and can be assumed to be 'exact'. According to the theorem of singular value decomposition (SVD) [12], the FRF matrix $\tilde{\mathbf{A}}$ can be decomposed using the factorization form

$$\tilde{\mathbf{A}} = \mathbf{U} \cdot \boldsymbol{\Sigma} \cdot \mathbf{V}^{H}, \tag{7}$$

where $\mathbf{U}$ and $\mathbf{V}$ are unitary matrices (also called Hermitian orthogonal), $\mathbf{V}^{H}$ is the adjoint matrix of $\mathbf{V}$, and $\boldsymbol{\Sigma}$ is a diagonal matrix whose elements are referred as the singular values of the matrix

$\tilde{\mathbf{A}}$. For the current case, $\mathbf{\Sigma}$ has the form

$$\mathbf{\Sigma} = \begin{bmatrix} \text{diag}(s_1, \ldots, s_n) \\ [0] \end{bmatrix}, \tag{8}$$

where s_1, s_2 …, s_n are non-negative singular values arranged in descending order, and diag(*) refers to a diagonal matrix with the elements in parentheses located on the main diagonal. Since this measurement noise will also propagate into the computed forces, the polluted forces can be found by replacing $\tilde{\mathbf{y}}$ in Eq. (4) with $\tilde{\mathbf{y}}_{\text{pol}}$ and using Eqs. (6) and (7). The forces identified using the polluted responses then have the form

$$\tilde{\mathbf{f}}_{\text{pol}} = \tilde{\mathbf{f}}_{\text{exact}} + \sum_{i=1}^{n} s_i^{-1}(\mathbf{u}_i^H \eta_i)\mathbf{v}_i, \tag{9}$$

where $\mathbf{u}_i$ refers to the column vector of $\mathbf{U}$, $\mathbf{V}_i$ is the ith column vector of $\mathbf{V}$, η_i is the ith element of $\tilde{\boldsymbol{\eta}}$, and s_i is the ith singular value of matrix $\tilde{\mathbf{A}}$. If $\tilde{\mathbf{A}}$ is ill-conditioned, the ratio between the largest and smallest singular values tends to be high and the division by the smallest singular values s_n, s_{n-1} … in Eq. (9) will amplify the measurement noise relative to the desired exact forces. A result of this amplified error will be a predicted force, $\tilde{\mathbf{f}}_{\text{pol}}$, that is far from the desired value $\tilde{\mathbf{f}}_{\text{exact}}$. One way to minimize the influence of noise amplification is to add a filter function $W_\alpha(s_i^2)$ for which $W_\alpha(s_i^2)s_i^{-1}$ approaches zero as s_i approaches zero [7]. To that end, the formulation

$$\tilde{\mathbf{f}}_\alpha = \tilde{\mathbf{f}}_{\text{exact}} + \sum_{i=1}^{n} W_\alpha(s_i^2)s_i^{-1}(\mathbf{u}_i^H \eta_i)\mathbf{v}_i \tag{10}$$

can be used, where the filter is defined as

$$W_\alpha(s_i^2) = \begin{cases} 1, & \text{if } s_i^2 > \alpha, \\ 0, & \text{if } s_i^2 < \alpha, \end{cases} \tag{11}$$

and α refers to the regularization parameter, which is a constant. The notation $\tilde{\mathbf{f}}_\alpha$ is used to represent the force computed from a regularized measured response that contains noise. This filter is known as the truncated singular value decomposition (TSVD) filter. Hence the TSVD-based LS scheme takes the final form

$$\tilde{\mathbf{f}}_\alpha = \tilde{\mathbf{f}}_{\text{exact}} + \sum_{i:s_i^2 > \alpha} s_i^{-1}(\mathbf{u}_i^H \eta_i)\mathbf{v}_i. \tag{12}$$

Since $W_\alpha(s^2)$ in Eq. (11) can only take on values of 0 or 1, the TSVD filter can be regarded as a step function. Because of this discontinuous behavior, the TSVD filter may in fact filter out useful structural dynamic information since it completely removes the smallest singular values, hence reducing the accuracy of the inversion in Eq. (4). Another option for reducing the effects of errors is the Tikhonov filter.

The Tikhonov filter is a continuous filter that has the form

$$W_\alpha(s^2) = \frac{s^2}{s^2 + \alpha}. \tag{13}$$

Based on this filter, the Tikhonov-based LS scheme formulation is

$$\tilde{\mathbf{f}}_{\alpha} = \tilde{\mathbf{f}}_{\text{exact}} + \sum_{i=1}^{n} \frac{s_i}{s_i^2 + \alpha} (\mathbf{u}_i^H \eta_i)\mathbf{v}_i. \tag{14}$$

In comparing Eq. (12) to Eq. (14), it is worth noting that the continuous property of the Tikhonov-based LS scheme suppresses noise in the structural responses while retaining more dynamic information than the TSVD-based LS scheme. As a result, the Tikhonov scheme has a tendency to be more accurate. Of course, the effectiveness of each of these approaches depends on the selection of the regularization parameter α.

The Morozov's discrepancy principle can be used to choose a proper regularization parameter if a priori estimation of the noise level in the measured structural responses is possible. This principle has a more desirable convergence property than the methods used in the work of Thite [8,9]. The difference between these principles is beyond the scope of this paper, and therefore won't be discussed in detail here. However, this difference is elaborated in Ref. [7]. According to this principle, the value selected for the regularization parameter α should be such that the residue between the regularized and non-regularized solutions equals the estimated noise norm ε [7]:

$$\left\| \tilde{\mathbf{A}}\tilde{\mathbf{f}}_{\alpha} - \tilde{\mathbf{y}}_{\text{pol}} \right\| \approx \varepsilon, \tag{15}$$

where

$$\varepsilon = \left\| \boldsymbol{\eta} \right\|_2. \tag{16}$$

In order to select the optimum regularization parameter for the enhanced LS schemes, a new formulation of this discrepancy principle is developed here. The portion of the response vector $\tilde{\mathbf{y}}_{\text{pol}}$ associated with the null space of $\tilde{\mathbf{A}}$, denoted by $\sum_{i=n+1}^{m} (\mathbf{u}_i^{\mathrm{T}} \tilde{\mathbf{y}}_{\text{pol}})^2$, cannot be resolved by any LS scheme. The discrepancy formulation of Eq. (15) can be reformulated for the TSVD-based LS scheme as

$$\sum_{i=k}^{n} (\mathbf{u}_i^{\mathrm{T}} \tilde{\mathbf{y}}_{\text{pol}})^2 \approx \varepsilon^2 - \sum_{i=n+1}^{m} (\mathbf{u}_i^{\mathrm{T}} \tilde{\mathbf{y}}_{\text{pol}})^2, \tag{17}$$

where α now satisfies the inequality $s_k^2 > \alpha \geqslant s_{k+1}^2$ and is used to truncate the series. It is worth noting at this point that normally the size of the FRF matrix is small, since typically only a few dynamic forces need to be identified. As a result, it is not necessary to obtain an extremely precise value for α. One only needs to find the largest s_k such that the inequality

$$\sum_{i=k}^{n} (\mathbf{u}_i^{\mathrm{T}} \tilde{\mathbf{y}}_{\text{pol}})^2 \leqslant \varepsilon^2 - \sum_{i=n+1}^{m} (\mathbf{u}_i^{\mathrm{T}} \tilde{\mathbf{y}}_{\text{pol}})^2 \tag{18}$$

is satisfied. Then α can simply be selected for the range noted for Eq. (17).

The regularization parameter α for the Tikhonov-based LS scheme can be chosen in a similar way such that it satisfies the approximate relationship

$$\sum_{i=1}^{n} \left\{ \left[1 - \frac{s_i^2}{s_i^2 + \alpha} \right] (\mathbf{u}_i^{\mathrm{T}} \tilde{\mathbf{y}}_{\text{pol}}) \right\}^2 \approx \varepsilon^2 - \sum_{i=n+1}^{m} (\mathbf{u}_i^{\mathrm{T}} \tilde{\mathbf{y}}_{\text{pol}})^2. \tag{19}$$

Depending on the method selected, one can apply Eq. (17) or Eq. (19) at each frequency to determine the required regularization parameter. However, by doing this, the computational costs tend to increase significantly because of these complicated filters and parameter selection processes. Hence, it is useful to find a criterion for the threshold of applying these enhanced LS schemes.

To address the issue of finding a threshold criterion, this research proposes using the second norm condition number of the rectangular FRF matrix $\tilde{\mathbf{A}}$. This norm, which has been found have a direct relationship with the error amplification effect in the inverse process [13], is defined as the ratio of the largest singular value to the smallest singular value

$$\kappa(\tilde{\mathbf{A}}) = \frac{s_1}{s_n}, \tag{20}$$

where $\kappa(\cdot)$ refers to matrix condition number. If $\tilde{\mathbf{A}}$ is ill-conditioned, then $\kappa(\tilde{\mathbf{A}})$ tends to be large. Here it is proposed that if the value of $\kappa(\tilde{\mathbf{A}})$ at the frequency of interest is larger than a threshold value of κ_{th}, which is pre-selected to be between 80 and 120, then an enhanced LS scheme should be applied to overcome any inversion singularity. At the other frequencies, where $\kappa(\tilde{\mathbf{A}})$ is less than the value of κ_{th}, the standard LS scheme is able to handle the force identification problem. The selection of the specific value of κ_{th} depends upon the preference of computational efficiency versus accuracy at each frequency. If κ_{th} is selected to be close to 80, then the preference is for accuracy. On the other hand, if κ_{th} is selected close to 120, then the preference is for computational efficiency. Although a specific single value for κ_{th} is not provided here, this range can be of use when trying to determine whether or not the enhanced LS scheme should be applied at a particular frequency. This criterion will be demonstrated in the numerical example section below, where the excitation frequency of the identified force will be assumed to be unknown. In those cases, either a conventional LS approach or an enhanced approach will be applied to each frequency component in the time-domain signal, with the particular approach depending on the value of the condition number at that frequency. The range of threshold values specified above is based on the results of simulations conducted in this research as well as observations made from a review of Thite's work [8,9] and can be applied to other cases.

Although the enhanced and conventional LS schemes are formulated to address errors associated with measurement of the structural response. For many dynamic force identification problems the FRF matrix $\tilde{\mathbf{A}}$ is not precisely known. For example, $\tilde{\mathbf{A}}$ may be polluted by measurement or modeling errors. Hence, there is a need to use a robust method for reducing the effects of errors in both the measured structural responses $\tilde{\mathbf{y}}_{\text{pol}}$ and the FRF matrix $\tilde{\mathbf{A}}$. One possible method, the total least-squares (TLS) scheme, has not been previously used in the area of force identification and is therefore discussed in the next section.

4. Total least-squares scheme

The TLS scheme is applied here to address the problem of errors present in both the FRF matrix and the structural response. The TLS scheme finds a solution by perturbing both the FRF matrix and the structural response vector with the minimum Frobenious norm of the augmented

matrix $[\Delta\tilde{\mathbf{A}}, \Delta\tilde{\mathbf{y}}]$, where $\Delta\tilde{\mathbf{A}}$ is the perturbation of the FRF matrix and $\Delta\tilde{\mathbf{y}}$ is the perturbation of structural responses. Although here it will be applied to the force identification case, the general TLS methodology can be found in Ref. [14].

The augmented matrix $\left[\tilde{\mathbf{A}}_{\text{pol}}, \tilde{\mathbf{y}}_{\text{pol}}\right]$ can be factorized by the SVD technique as

$$\left[\tilde{\mathbf{A}}_{\text{pol}}, \tilde{\mathbf{y}}_{\text{pol}}\right] = \bar{\mathbf{U}} \cdot \bar{\mathbf{\Sigma}} \cdot \bar{\mathbf{V}}^H, \tag{21}$$

where $\bar{\mathbf{U}}$ and $\bar{\mathbf{V}}$ are unitary matrices. Similar to the approach used earlier, $\bar{\mathbf{\Sigma}}$ has the form

$$\bar{\mathbf{\Sigma}} = \begin{bmatrix} \text{diag}\,(\bar{s}_1, \ldots, \bar{s}_{n+1}) \\ [0] \end{bmatrix}, \tag{22}$$

where $\bar{s}_i$ is the ith singular value of the augmented matrix $\left[\tilde{\mathbf{A}}_{\text{pol}}, \tilde{\mathbf{y}}_{\text{pol}}\right]$. Here, the $\bar{\mathbf{V}}$ matrix can be partitioned as

$$\bar{\mathbf{V}} = \begin{matrix} \\ k \end{matrix} \begin{matrix} \begin{pmatrix} \bar{\mathbf{V}}_{\mathbf{11}} & \bar{\mathbf{V}}_{\mathbf{12}} \\ \bar{\mathbf{V}}_{\mathbf{21}} & \bar{\mathbf{V}}_{\mathbf{22}} \end{pmatrix}^{n}_{1} \\ n-k+1 \end{matrix}, \tag{23a}$$

where k is the regularization parameter. Note that integer k is used to represent the TLS regularization parameter while α is used for the LS scheme.

Then, the TLS solution $\tilde{\mathbf{f}}_{\text{tls}}$ is computed as

$$\tilde{\mathbf{f}}_{\text{tls}} = -\bar{\mathbf{V}}_{12}\,\bar{\mathbf{V}}_{22}^{+}, \tag{23b}$$

where $\bar{\mathbf{V}}_{22}^{+}$ refers to the pseudo-inverse of $\bar{\mathbf{V}}_{22}$, as defined in Eq. (5). If the augmented matrix $[\tilde{\mathbf{A}}_{\text{pol}}, \tilde{\mathbf{y}}_{\text{pol}}]$ is ill-conditioned, which can be quantified by a large value of $\kappa([\tilde{\mathbf{A}}_{\text{pol}}, \tilde{\mathbf{y}}_{\text{pol}}])$ as defined in Eq. (20), a TLS regularization parameter $k>1$ should be selected. Otherwise, choose $k=1$. Here, it is worth noting that in the area of mathematics, if $k>1$, the algorithm is also referred as a truncated TLS scheme [14].

The choice of the regularization parameter is referred to as the stopping criterion in Ref. [14] based on the theory that the regularization level should be such that the norm of the TLS residue matrix equals the a priori known error

$$\left\|\Delta\tilde{\mathbf{A}}, \Delta\tilde{\mathbf{y}}\right\|_F \approx \varepsilon. \tag{24}$$

Golub and Fierro studied the numerical differences between the TLS scheme and the LS scheme in Refs. [15,16]. When expressing those results in terms of the force identification case, one can conclude that under the condition that $\tilde{\mathbf{y}}_{\text{pol}}$ is not highly incompatible with the column space of $\tilde{\mathbf{A}}_{\text{pol}}$, that is, $\tilde{\mathbf{y}}_{\text{pol}}$ can be approximated using linear combination of column vectors of $\tilde{\mathbf{A}}_{\text{pol}}$, and the response is oriented along the vectors corresponding with the smallest singular values of $\tilde{\mathbf{A}}_{\text{pol}}$, the TLS scheme works much better than the LS schemes. It is worth noting that these results are restricted to numerically solvable problems.

It is also worth noting that the TLS scheme is sensitive to the magnitude of the input forces. This is evident when one considers that the TLS scheme is trying to get the minimum Frobenius-

norm of the augmented matrix $[\Delta\tilde{\mathbf{A}}, \Delta\tilde{\mathbf{y}}]$, in which $\Delta\tilde{\mathbf{y}}$ has a direct relationship with the magnitude of these forces. Hence, if the amplitude of the force, for example, increases by a factor of 1000, then the TLS scheme is more likely to reduce the effect of errors in the structural response. Otherwise, if the force amplitudes are small, the TLS scheme is more likely to reduce the effect of errors in the FRF matrix. One could, of course, use the approach presented by Golub [15] in which the augmented matrix is pre- and post-multiplied by appropriately selected diagonal weighting matrices. Unfortunately, searching for the optimal weighting matrices at each frequency for a broad-band force identification problem can be extremely computationally expensive. One approximate solution might be to select the weighting matrices such that the singular value of the weighted response is comparable to the singular values of the weighted FRF matrix. However, further research on this approach is needed to validate its applicability and accuracy. As a result, issues related to the magnitudes of the input forces are not addressed here and will the subject of future research.

Although the methods for improving force reconstruction described earlier are applied here to address some issues that commonly arise in force identification problems, it is beneficial to examine their efficiency through some numerical examples. In the numerical examples described below, two example cases at different frequencies, each containing two forces, are examined with the conventional LS approach. Then, the structural responses are perturbed by random errors and the enhanced LS schemes described in Section 3 are used to identify the dynamic forces. The results computed from the enhanced LS schemes are compared with those from the conventional LS scheme described in Section 2. Finally, both the FRF matrix and the structural responses are perturbed by random errors and the TLS scheme developed in Section 4 is used to identify the dynamic forces. In order to evaluate the effectiveness of the TLS scheme, the identified results are compared with those of the conventional and enhanced LS scheme.

5. Numerical applications

In the following numerical examples, two sinusoidal forces acting on a free–free beam will be identified by using the force identification techniques described above. The excitation points are selected to be near the end of the beam as shown in Fig. 1. The free–free beam is made of steel with an overall dimension of $50 \times 50 \times 1000\,\text{mm}^3$, where the last dimension is the length. The material properties of the beam are listed in Table 1. By simulating the response of the beam using a finite element (FE) method, the responses of the beam at five locations are computed. These computed responses are used as virtual accelerometer measurements, numbered 1 through 5, which will serve for the purposes of measured responses in these examples. More details regarding these 'virtual measurements' is provided later. The measurement locations are selected to span the first and the second flexural modes to improve the quality of the identified results.

Consider the two different excitation cases denoted by Case A, where $F_1(t) = \sin(200\pi t)$ and $F_2(t) = -2 \times F_1(t)$, and Case B, where $F_1(t) = \sin(520\pi t)$ and $F_2(t) = -2 \times F_1(t)$.

The difference in these two cases is that in Case A the forcing frequency of 100 Hz is not near any natural frequency of the beam, whereas in Case B the excitation frequency of

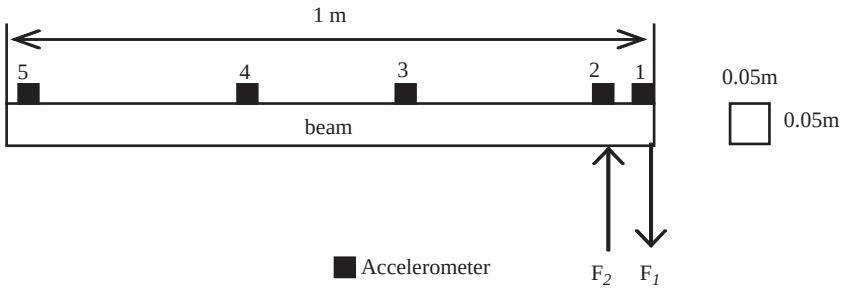

Fig. 1. Schematic of a free–free beam system used in force identification. Two forces F_1 and F_2 and five virtual accelerometers located on the beam.

Table 1
The material properties, natural frequencies and damping ratio of the free–free beam

Young's modulus (GPa)		206.8
Density (kg/m^3)		7820
Poison's ratio		0.29
Computed natural frequencies (Hz)	First mode	261.4
	Second mode	708.1
Modal damping ratio	First mode	1%
	Second mode	1%

260 Hz is near the first natural frequency of the beam, which is approximately 261 Hz.Note that these excitation configurations impose a net force as well as a net moment near the end of the beam.

As noted above, the structural responses for each of these cases were obtained using a FE method. One might use analytic methods to obtain these responses for such a simple structure. The application of these analytical methods on complicated structures, which are common in most practical engineering problems, is often impossible. Hence the FE method is preferred in this paper since it is often used as a correlation method in real practice. Furthermore, the FE method is not exact. For the cases studied, the beam was meshed using 400 eight-node solid elements so that two rigid body modes and two flexural modes could be computed. A modal summation method was used to obtain the FRF matrix in the frequency domain and the structural response in the time domain. Then, to produce the virtual experimental data from these computed results, the response was sampled at a frequency of 8192 Hz, and a simulated 1 s sample duration of 'measurement' data was obtained. In the force identification process, of course, the excitation frequency of the force is not initially known. Then, the force identification approach was applied in some of the cases described below, where a measurement error was also introduced in the response data.

5.1. Least-squares solutions

First, the conventional LS scheme was used to identify the dynamic forces with the clean FE results used as the measured responses. The results of the identified dynamic force F_1 for Cases A and B are shown in Figs. 2 and 3, respectively. For both the cases shown, the time histories of the identified forces F_1 match the actual dynamic forces quite well. However, further examination of the identified force in the frequency domain reveals that the peak of F_1 in both cases deviates slightly from the exact solution that should be around 4000 N/Hz. The peak of the identified force is less than the exact solution and the dynamic energy smears over adjacent frequencies, as shown in the frequency-domain plots. These deviations are due to the fact that: (1) a rectangular window was used to obtain the time-domain responses, which might cause signal leakage and deviation in the frequency domain, and (2) numerical errors associated with data processing, and (3) the FFT is used, which is not always as accurate as the continuous FT. Furthermore, since the structural response tends to be very large near resonances, it is not surprising that the smearing effect for Case B is more pronounced than for Case A. Although not shown, the identified force F_2 also matches the exact solution in the time domain for both cases and in the frequency domain the amplitude deviates from the exact solution in a similar way as F_1. These figures demonstrate that the conventional LS scheme is able to identify the dynamic forces correctly even when small modeling errors, which could be taken as very small measurement errors, are present in the structural responses. Furthermore, the success of the LS scheme also validates that this problem

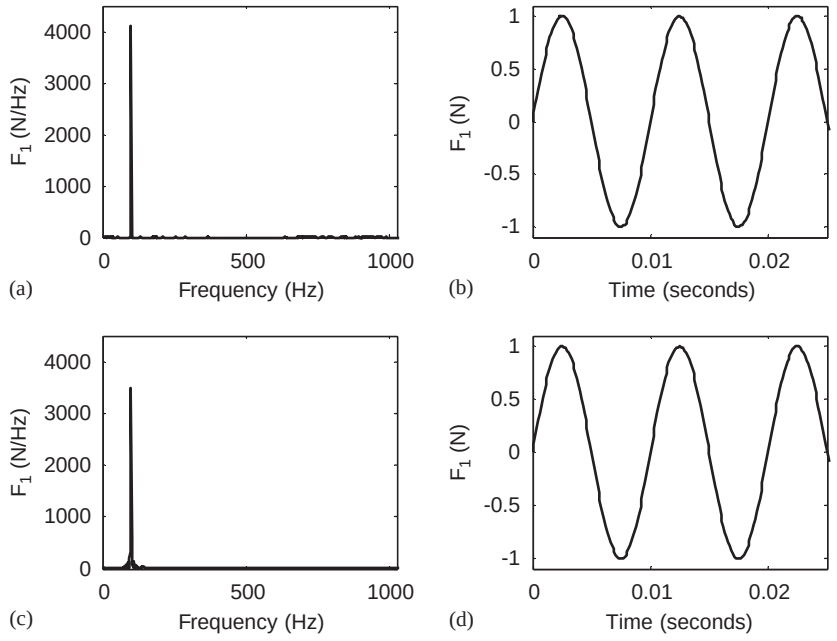

Fig. 2. Case A. Comparison of exact force F_1 in the (a) frequency and (b) time domains to F_1 identified with the LS scheme in the (c) frequency and (d) time domains.

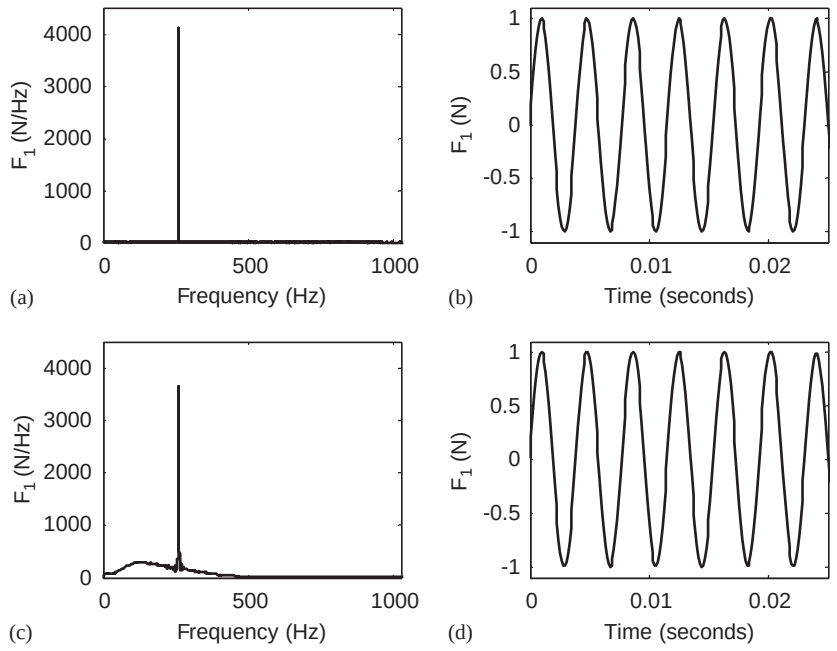

Fig. 3. Case B. Comparison of exact F_1 in the (a) frequency and (b) time domains to F_1 identified with the LS scheme in the (c) frequency and (d) time domains.

is numerically solvable. Analysis of the smallest singular values of the FRF matrix, as shown in Fig. 4, indicates that the values are much larger than computer precision (2.22×10^{-16}). Hence for the cases considered in this paper, the force identification problem is numerically solvable for all the frequencies. At this point, it is interesting to note that if the number of dynamic forces is increased or any rigid body mode are missing from the measured response, of a constrained beam for example, the condition of the FRF matrix might be very ill-conditioned near any resonances. For these cases, the smallest singular value tends to be below the computer precision, making the force identification process near resonances impossible [17].

In both the cases considered, the errors in the FE method are pretty small compared with real experiments. To examine the effect of random response noise on the accuracy of identified forces for both Cases A and B, an amplitude Gaussian noise matrix $\Delta\mathbf{y}$ and a phase Gaussian noise matrix $\Delta\varphi$ were introduced into the amplitudes and phases of the measured structural responses, respectively, as

$$\mathbf{y}_i^{\text{noisy}} = \mathbf{y}_i \cdot \Delta\mathbf{y}_i \cdot \mathrm{e}^{\mathrm{j}\Delta\varphi}. \tag{25}$$

In this equation, $\mathbf{y}_i$ refers to the numerical measurement of the ith simulated accelerometer. $\Delta\mathbf{y}_i$ is the Gaussian noise with a mean equal to unity and a standard deviation equal to 0.05. Also $\Delta\varphi$ has a mean of zero and a standard deviation equal to 0.09 rad (5°).

The conventional LS scheme was applied with the errors described above and the identified forces are compared with the exact forces for Cases A and B in Figs. 5 and 6, respectively. In order

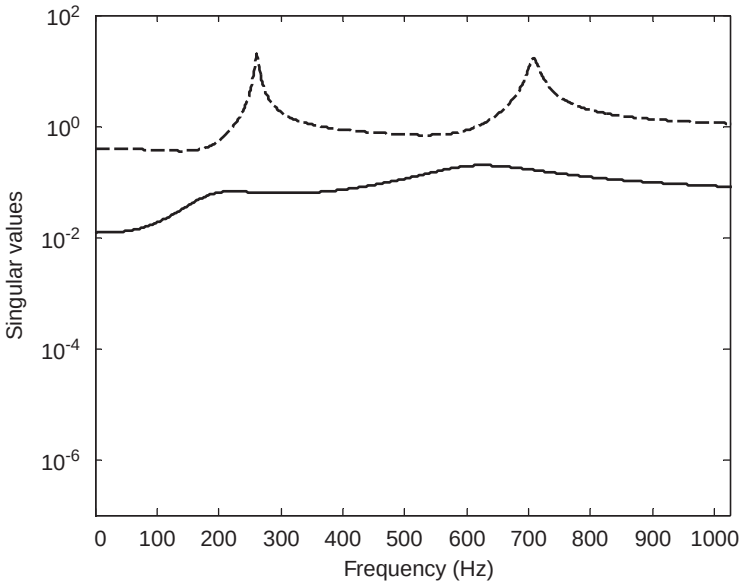

Fig. 4. Singular values of the FRF matrix at each frequency (---, first singular value, — second singular value).

to quantify the errors between the exact solution and the identified solution, the discrepancy ξ_t [11] is found using the relationship

$$\xi_t = \frac{\sum_i \left| f^{\text{identified}}(t_i) - f^{\text{exact}}(t_i) \right|}{\sum_i \left| f^{\text{exact}}(t_i) \right|} \times 100\%, \tag{26}$$

where $f^{\text{identified}}(t_i)$ and $f^{\text{exact}}(t_i)$ refer to the identified and exact forces at time t_i, respectively. For Case A in Fig. 5, in both the time domain and the frequency domain, the dynamic forces computed from the LS scheme match the exact forces quite well. For Case B in Fig. 6, the structural measurement errors are significantly amplified by the LS scheme. In the frequency domain, the amplitude peak of the identified force F_1 is more than 5 times the exact force, whereas the amplitude peak of the identified force F_2 is more than 4 times the exact force. These spurious peaks in the frequency domain result in unacceptable identified forces, as demonstrated in the time-domain plots of Fig. 6. Further examination of ξ_t in Table 2 shows that for the polluted responses, in Case A, ξ_t for F_1 is 0.4 and for F_2 is 0.3, whereas in Case B, ξ_t for F_1 is 4.51 and ξ_t for F_2 is 3.57. It is worth noting that in both cases, the random errors in the responses are amplified near the resonances. However, since the input error level is defined to be proportional to the amplitude of the responses, which is quite reasonable in real applications, the error levels for Cases A and B are quite different. In Case A, the structural response energy is concentrated at 100 Hz, where the FRF matrix tends to be well-conditioned. In contrast, for Case B, the structural responses energy is concentrated at 260 Hz, where the FRF matrix tends to be ill-conditioned.

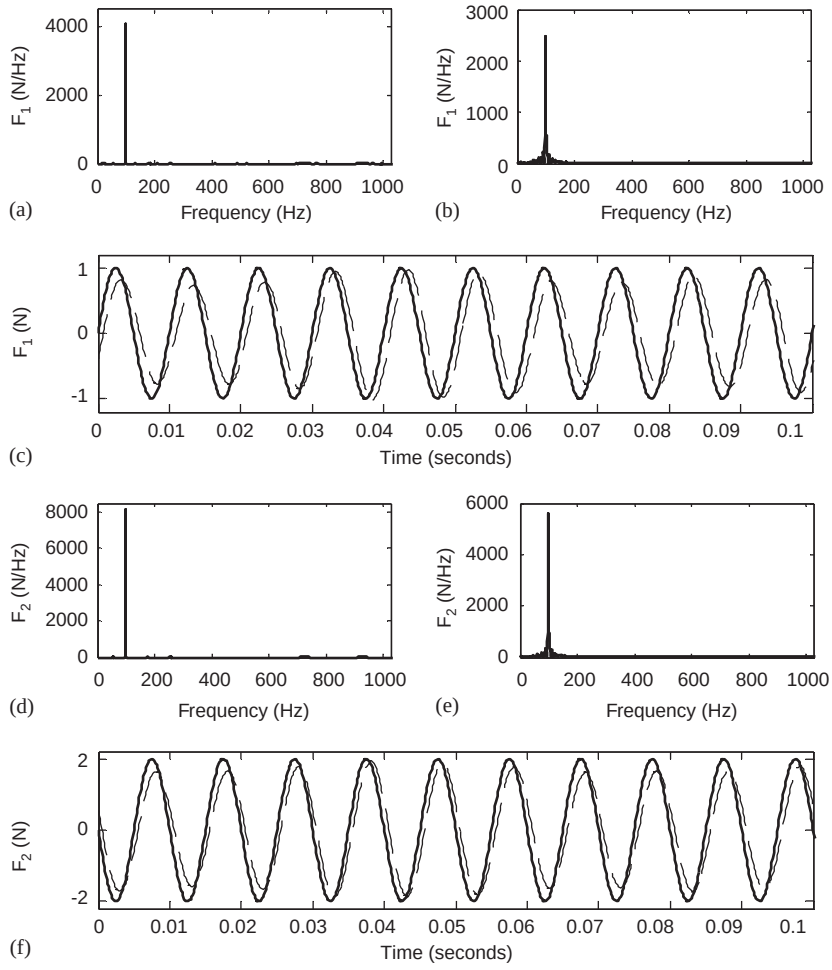

Fig. 5. Case A with Gaussian noise. Comparison of LS scheme identified and exact F_1: (a) Exact solution and (b) identified solution in the frequency domain, (c) exact solution (—) and identified solution (- - -) in the time domain. Same for F_2: (d) exact solution and (e) identified solution in the frequency domain, (f) exact solution (—) and identified solution (- - -) in the time domain.

Therefore, one would expect for Case B that the measurement error tends to be much larger than for Case A and that these errors are significantly amplified in the inverse process, thus making the LS scheme inadequate. In order to clearly illustrate the effect of regularization methods described above, these methods are only applied to Case B.

The quantification of the effect of error amplification at each frequency can be described by the matrix condition number $\kappa(\tilde{\mathbf{A}})$ given in Eq. (20). In Fig. 7, $\kappa(\tilde{\mathbf{A}})$ is shown over the frequency range of 0–1025 Hz.The largest increases in $\kappa(\tilde{\mathbf{A}})$, corresponding to the potential for error amplification, are observed when the frequency is located in the vicinity of the resonances. Here, the criterion proposed in the Section 4 is applied and a preference is placed on computational efficiency. As a

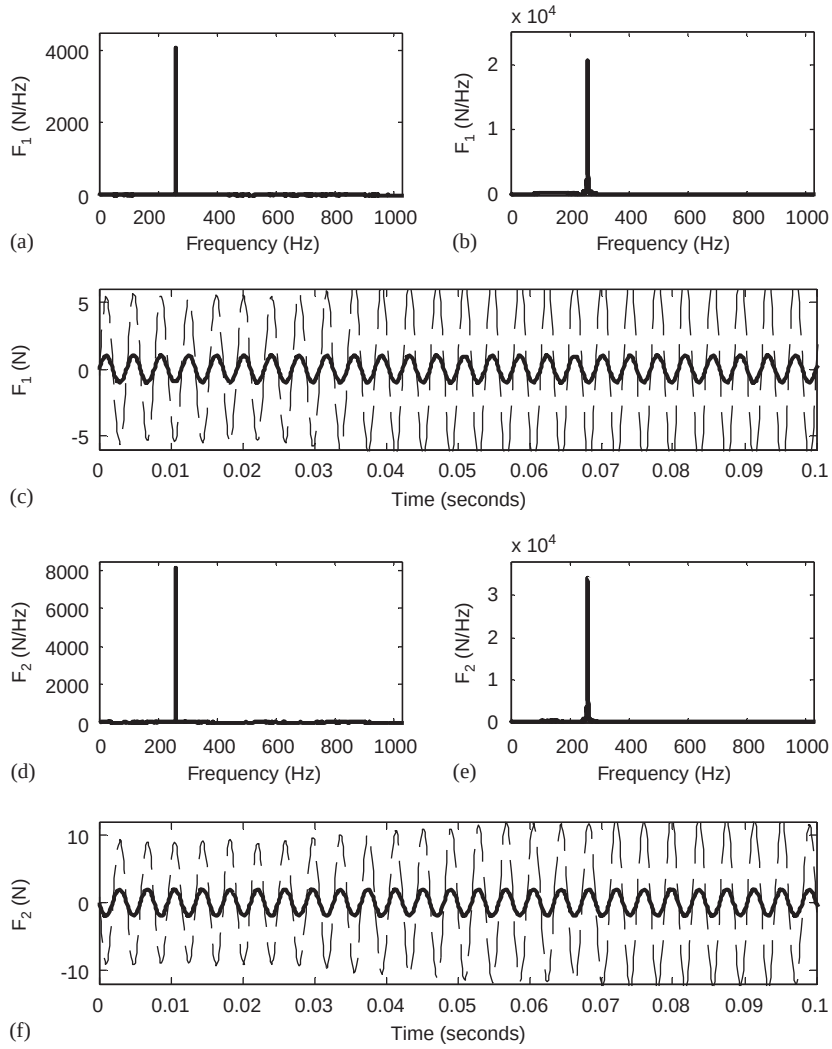

Fig. 6. Case B with Gaussian noise. Comparison of LS scheme identified and exact F_1: (a) exact solution and (b) identified solution (Peak = 21,000 N/Hz) in the frequency domain, (c) exact solution (—) and identified solution (- - -) in the time domain. Same for F_2: (d) exact solution and (e) identified solution (Peak = 34,000 N/Hz) in the frequency domain, (f) exact solution (—) and identified solution (- - -) in the time domain.

result, a threshold value of 85 is selected for κ_{th}. Since the excitation frequency is assumed to be unknown, the identification method is applied to all of the frequency components present in the time-domain data. For those components at which the condition number of the FRF matrix exceeds κ_{th}, a regularization scheme is applied to reduce the effect of response errors. For all of the other frequency components, where the condition number is below this threshold, the conventional LS approach is used.

Table 2
Comparison of discrepancy ξ_t of LS, TSVD-based LS, and Tikhonov-based LS (duration = 1 s)

Case	LS		TSVD	Tikhonov
A	From original responses	From polluted responses	From polluted responses	From polluted responses
Force F_1	0.004	0.4		
Force F_2	0.004	0.3		
B				
Force F_1	0.06	4.51	1.26	0.48
Force F_2	0.04	3.57	1.00	0.37

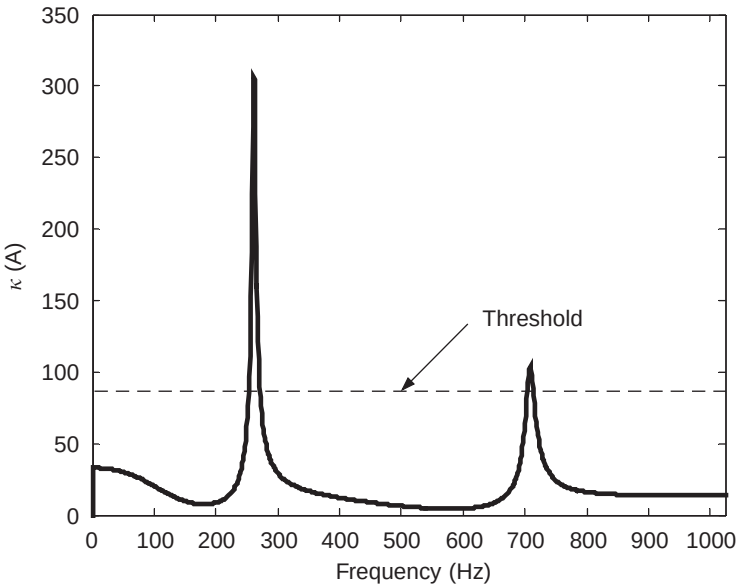

Fig. 7. Condition number $\kappa(A)$ as a function of frequency.

5.2. TSVD and Tikhonov filter solutions

To investigate the effects of regularizing the error amplification effect in Case B, the TSVD-based LS scheme was applied at the frequencies where the above criterion is satisfied. A further check of the regularization parameters, such that $(\mathbf{u}_2^{\mathrm{T}}\tilde{\mathbf{y}}_{\mathrm{pol}})^2 \leqslant \varepsilon^2 - \sum_{i=3}^{5}(\mathbf{u}_i^{\mathrm{T}}\tilde{\mathbf{y}}_{\mathrm{pol}})^2$ is satisfied, ensures that the solution is not over-regularized. The forces identified from the responses containing the errors described above are shown in Fig. 8 for this approach. Compared with the results in Fig. 6, the accuracy of the results from TSVD-based LS scheme is considerably improved over the conventional LS scheme in both the frequency domain and the time domain. In the frequency

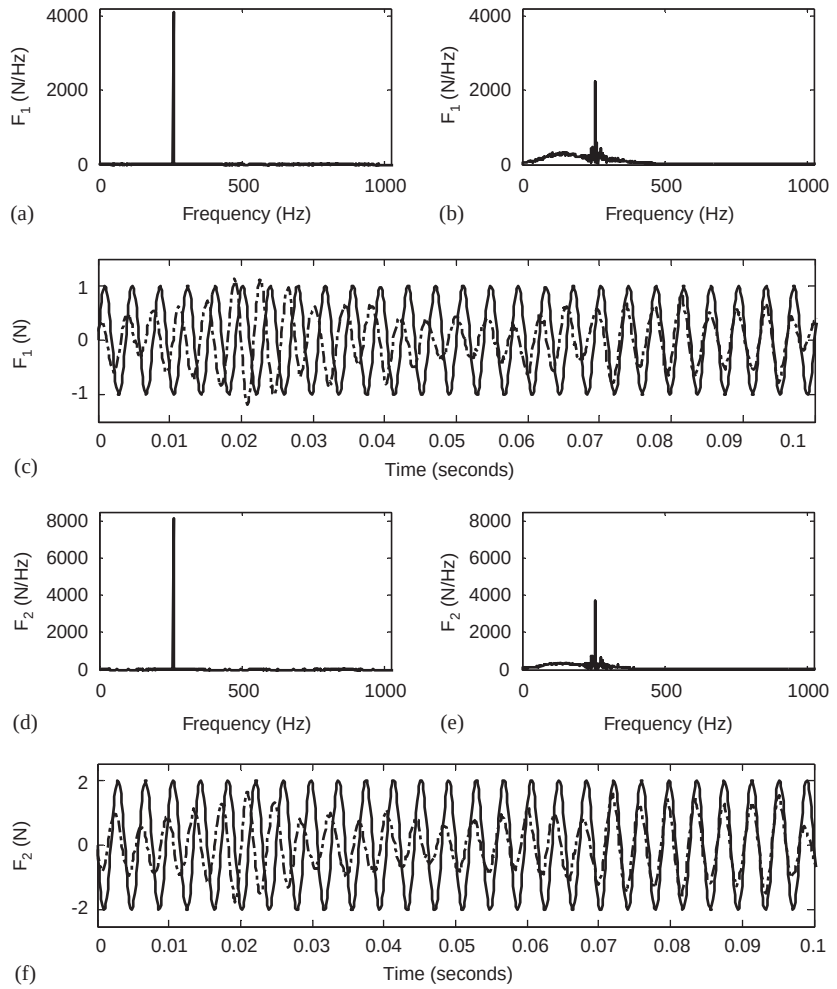

Fig. 8. Comparison of TSVD-based LS scheme identified and exact F_1: (a) exact solution and (b) identified solution in the frequency domain, (c) exact solution (—) and identified solution (- - -) in the time domain. Same for F_2: (d) exact solution and (e) identified solution in the frequency domain, (f) exact solution (—) and identified solution (- - -) in the time domain.

domain, the spurious large peak near 260 Hz for the conventional approach (Fig. 6) is regularized to an acceptable level (Fig. 8). Note that for improved plotting resolution, the scales on the plot are not the same. Study of the discrepancy ξ_t, shown in Table 2, illustrates the effect of applying the TSVD-based LS scheme. The discrepancies ξ_t of and F_2 are both reduced by over 70%. However, the regularized amplitude peak is a little bit lower than the exact solution and in the time domain the identified forces do not match the exact force well, which is due to the fact that TSVD filter is a discrete filter that tends to nullify some important dynamic information. It can be deduced that for the small-sized FRF matrix (in this case, the FRF matrix is 5×2), the effect of this missing information is more pronounced. Hence, the accuracy of this scheme is not

satisfactory for the numerical example considered. As a result, it is useful to consider other approaches for improving the results.

Next, a Tikhonov-based LS scheme is applied. The regularization parameters are computed by Morozov's discrepancy principle in Eq. (19). In order to find the optimum parameters, the function $D(\alpha)$ is defined such that

$$D(\alpha) = \sum_{i=n+1}^{m} (\mathbf{u}_i^{\mathrm{T}} \tilde{\mathbf{y}}_{\mathrm{pol}})^2 + \sum_{i=1}^{n} \left\{ \left[1 - \frac{s_i^2}{s_i^2 + \alpha} \right] (\mathbf{u}_i^{\mathrm{T}} \tilde{\mathbf{y}}_{\mathrm{pol}}) \right\}^2 - \varepsilon^2. \tag{27}$$

In Fig. 9, $D(\alpha)$ is plotted as a function of the regularization parameter α at 260 Hz.The optimum regularization parameter corresponds to the zero of the curve $D(\alpha)$. Table 3 lists the Tikhonov-based scheme regularization parameters computed using the same approaches for other frequencies near the first resonance. The identified forces using the Tikhonov-based LS scheme are illustrated in Fig. 10. A significant accuracy improvement of the identified forces is observed when compared with the results from the TSVD-based LS scheme of Fig. 8. This improvement in accuracy is due to the fact that the Tikhonov filter is a continuous function that is able to retain more useful dynamic information. The advantage of the Tikhonov-based LS scheme over the TSVD-based LS scheme is illustrated in Table 2, where the discrepancy ξ_t of F_1 is reduced by an additional 60% when using the Tikhonov scheme. The discrepancy ξ_t of F_2 is also reduced by an additional 60%. Clearly the improvements are much more dramatic for this case.

The above computational results show that if both the TSVD and Tikhonov filters are applied appropriately, the TSVD- and Tikhonov-based LS schemes are able to overcome the error

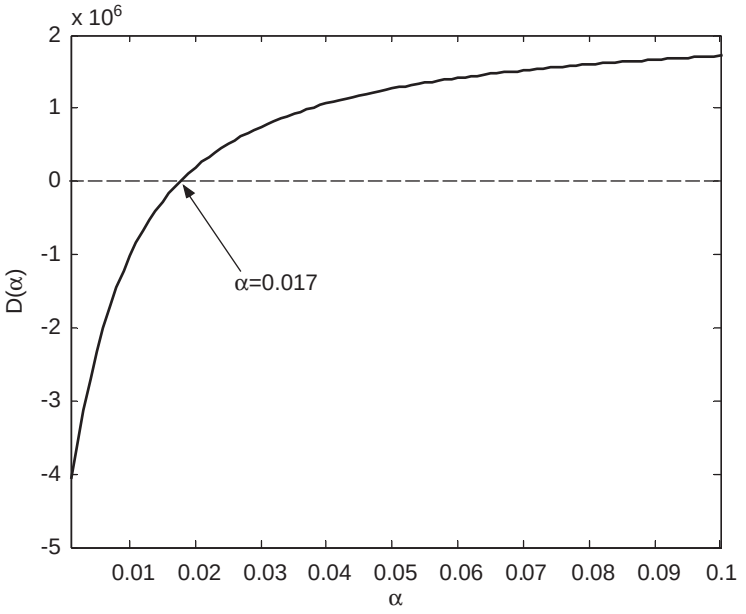

Fig. 9. Regularization parameter selection function $D(\alpha)$ at 260 Hz.

Table 3
Regularization parameters for Tikhonov-based LS scheme (Case B)

Frequency (Hz)	255	256	257	258	259	260	261	262
Parameter value	3.02	6.2	0.012	26.4	34.2	0.017	49.8	0.085
Frequency (Hz)	263	264	265	266	267	268	269	
Parameter value	0.017	25.4	0.013	6.6	10.8	11.8	6.77	

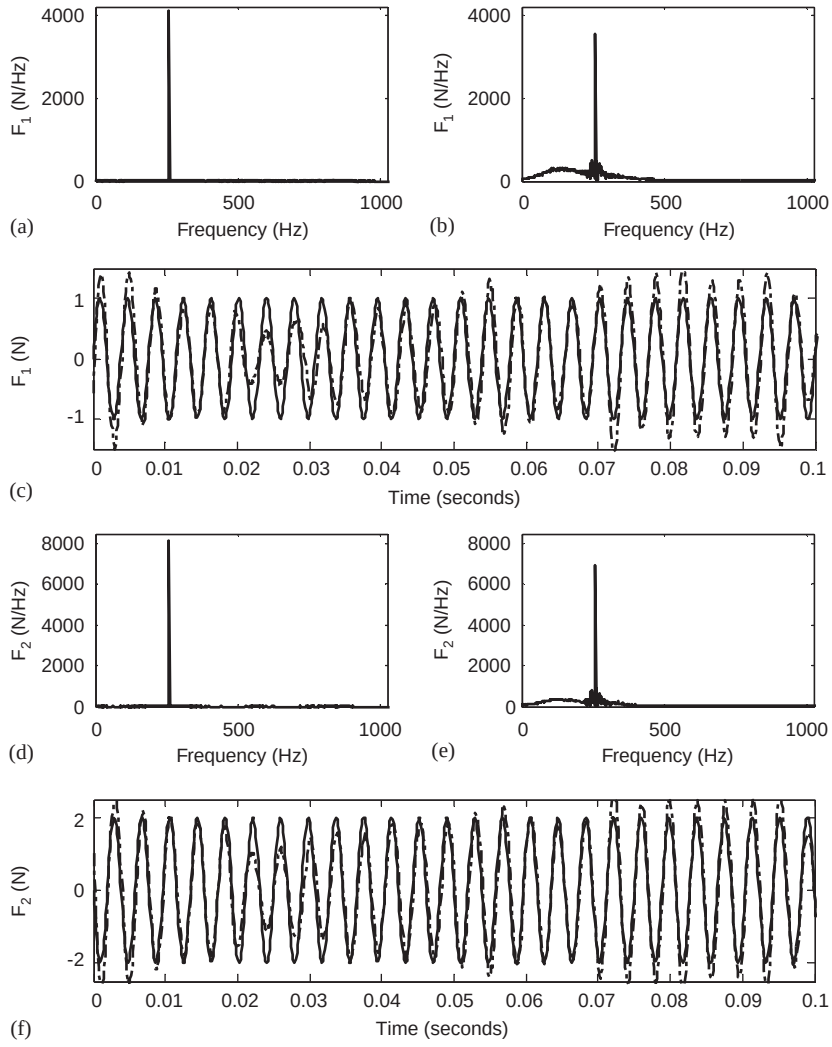

Fig. 10. Comparison of Tikhonov-based LS scheme identified and exact F_1: (a) exact solution and (b) identified solution in the frequency domain, (c) exact solution (—) and identified solution (- - -) in the time domain. Same for F_2: (d) exact solution and (e) identified solution in the frequency domain, (f) exact solution (—) and identified solution (- - -) in the time domain.

amplification problems inherent in conventional LS schemes and thereby the dynamic forces are identified more accurately. Unfortunately, an important limitation of these approaches is that they are based on the LS scheme, which works under the implicit assumption that the FRF matrix is not polluted. In some cases, FRF matrices are polluted by relatively large modeling and experimental errors. To further investigate methods for increasing the accuracy of the identified forces, the TLS scheme is applied to a case with both polluted responses and errors in the FRF matrix.

5.3. TLS scheme solutions

In the following examples, both the structural responses and the FRF matrix are subject to pollutions. The same level of errors is introduced into the structural responses as in the previous simulations. Furthermore, a 3% multiplicative Gaussian noise and a 0.06 rad added Gaussian noise are introduced into the FRF matrixes in order to simulate errors. For Case A, a sample solution by means of the conventional LS and the TLS schemes are compared with the exact solutions in Fig. 11. The solutions by both schemes match the exact solution pretty well. Furthermore, it can be seen that in general, the TLS scheme does a better job than the LS scheme. The discrepancy ξ_t of TSVD scheme and TLS scheme were computed to compare the identification deviations in the time domain. The discrepancy ξ_t of force F_1 and force F_2 are reduced from 0.60 to 0.52 and from 0.34 to 0.30, respectively, by using the TLS scheme.

Finally, consider Case B with the same errors added into the system. A sample solution by means of the LS and TLS schemes is compared with the exact solutions in Fig. 12. The identification results by the LS scheme are not near as good as in Case A. This is due to the fact that near resonances, the errors in both the FRF matrix and the responses may produce large errors in the identified results [5]. In the figure, the forces identified with the LS scheme cannot be distinguished clearly as sinusoidal forces, whereas the identified forces by the TLS scheme matches the exact solution well. Consequently, the identified dynamic forces computed by the TLS scheme are much improved. As before, the discrepancy ξ_t by LS and TLS schemes were computed to compare these results. The discrepancy ξ_t of the dynamic force F_1 when switching from the LS scheme to the TLS scheme is reduced from 1.11 to 0.94, respectively, and the discrepancy ξ_t of dynamic force F_2 is reduced from 0.88 to 0.72. In the figure, the phase-shift phenomena are due to the fact that random phases of the noise were amplified near resonance. Since some of this noise is intermingled with actual dynamic information, the influence of noise cannot be completely discarded by the TLS scheme.

The above simulations illustrate the fact that the TLS scheme works better than the LS scheme when both the FRF matrix and responses are polluted by errors. This improvement is due to the fact that the LS scheme is formulated under the assumptions that the FRF matrix is not polluted; whereas, the TLS scheme is formulated to simultaneously address the errors in both the FRF matrix and the responses. Further study of the numerical results shows that near resonances, the errors in the FRF matrix cause the LS scheme to fail. This phenomenon was also noticed in the work of Fabunmi [5]. Unfortunately, no solution was proposed in his work to address this problem.

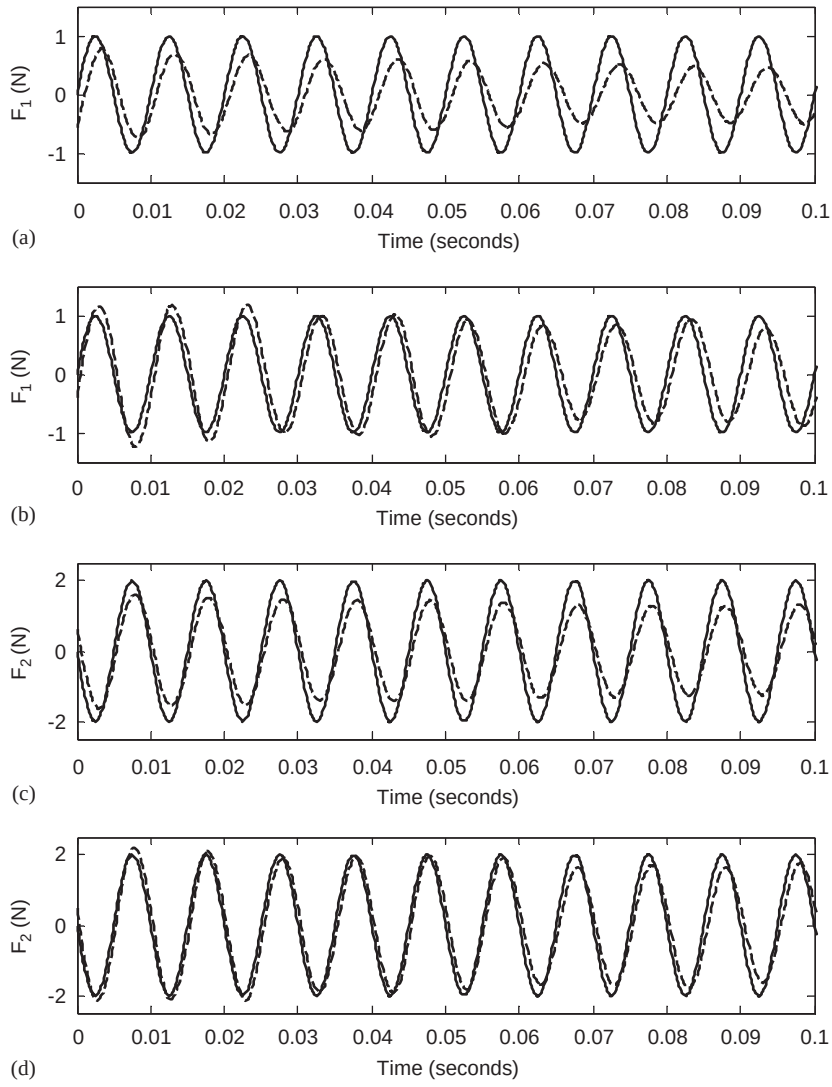

Fig. 11. Case A with response and FRF matrix errors. F_1: (a) —, exact solution; - - -, LS solution; (b) —, exact solution; - - -, TLS solution; F_2: (c) —, exact solution; - - -, LS solution; (d) —, exact solution; - - -, TLS solution.

6. Conclusion

In this work, various approaches were studied for force identification problems. To address the numerical instability near resonances, existing approaches that use TSVD and Tikhonov filters in the LS scheme were reviewed. Both regularization methods increase the accuracy of the LS scheme provided the problem is numerically solvable. The primary difference is that the TSVD filter is a discrete filter, whereas the Tikhonov filter is a continuous filter. Hence, the Tikhonov filter retains more dynamic information than the TSVD filter. The numerical results showed the

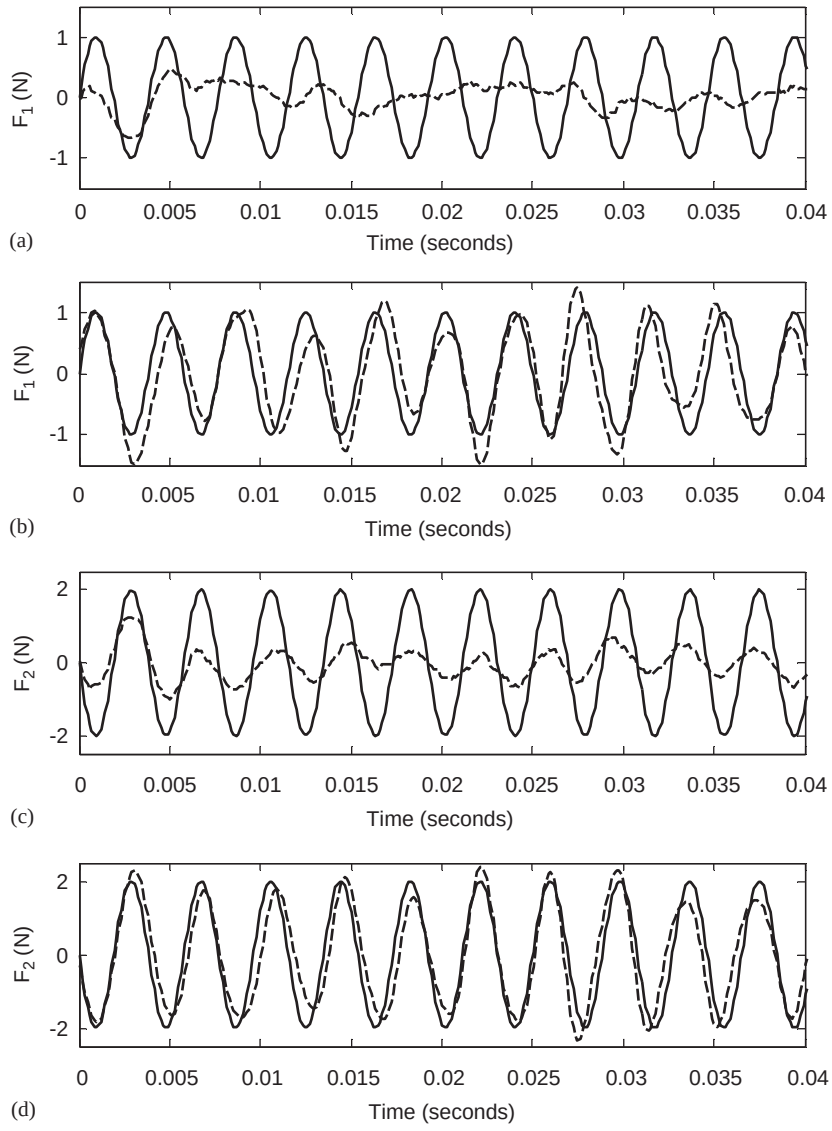

Fig. 12. Case B with response and FRF matrix errors. F_1: (a) —, exact solution; - - -, LS solution; (b) —, exact solution; - - -, TLS solution; F_2: (c) —, exact solution; - - -, LS solution; (d) —, exact solution; - - -, TLS solution.

significant advantage of the Tikhonov filter over the TSVD filter when the size of FRF matrix is small. This difference has not been noted by any previous article, thus making it quite difficult to choose an optimum filter for the conventional LS scheme. Rather than using the parameter selection principles described in some of previous works noted, a Morozov's discrepancy principle, which has a higher convergent rate than the other principles, was applied to select the optimum regularization parameters. Since these regularization filters require additional computation time, a criterion for applying the enhanced LS schemes was proposed in this work.

It was demonstrated that these complicated schemes are only necessary near the structural resonances. Finally, since both the FRF matrix and response vector can be polluted by measurement and modeling errors in real applications, a TLS scheme was developed here to reduce the effects of these errors. The theoretical and numerical comparison between the LS scheme and the TLS scheme showed that under certain conditions, the TLS scheme is able to give a much better result when both the transfer function matrix and the response data contains errors.

References

[1] K.K. Stevens, Force identification problems—an overview, *Proceedings of the SEM Spring Conference on Experimental Mechanics*, Houston, 1987.
[2] W.G. Bartlett Jr., F.D. Flannelly, Modal verification of force determination for measuring vibratory loads, *Journal of American Helicopter Society* 24 (2) (1979) 10–18.
[3] N. Okubo, S. Tanabe, T. Tatsuno, Identification of forces generated by a machine under operating condition, *The International Modal Analysis Conference*, 1985.
[4] J.A. Fabunmi, Modal constraints on structural dynamic force determination, *Journal of the American Helicopter Society* 30 (4) (1985) 48–54.
[5] J.A. Fabunmi, Effects of structural modes on vibratory force determination by the pseudoinverse technique, *AIAA Journal* 24 (3) (1986) 504–509.
[6] P.C. Hansen, *Rank-deficient and Discrete Ill-posed Problems*, SIAM, Philadelphia, 1998.
[7] C.R. Vogel, *Computational Methods for Inverse Problems*, SIAM, Philadelphia, 2002.
[8] A.N. Thite, D.J. Thompson, The quantification of structure-borne transmission paths by inverse methods—part 1: improved singular value rejection methods, *Journal of Sound and Vibration* 264 (2) (2003) 411–431.
[9] A.N. Thite, D.J. Thompson, The quantification of structure-borne transmission paths by inverse methods—part 2: use of regularization techniques, *Journal of Sound and Vibration* 264 (2) (2003) 433–451.
[10] B.J. Dobson, E. Rider, A review of the indirect calculation of excitation forces from measured structural response data, *Proceedings of the Institution of Mechanical Engineers. Part C: Journal of Mechanical Engineerings Science* 204 (1990) 69–75.
[11] L. Yu, T.H.T. Chan, Moving force identification based on the frequency–time domain method, *Journal of Sound and Vibration* 261 (2) (2003) 329–349.
[12] G.H. Golub, *Matrix Computation*, Johns Hopkins University Press, Battimore, MD, 1989.
[13] S.E.S. Karlsson, Identification of external structure loads from measured harmonic responses, *Journal of Sound and Vibration* 196 (1) (1996) 59–74.
[14] R.D. Fierro, G.H. Golub, P.C. Hansen, D.P. O'Leary, Regularization by truncated total least squares, *SIAM Journal on Scientific Computing* 18 (1997) 1223–1241.
[15] G.H. Golub, C.F.V. Load, An analysis of the total least squares problem, *SIAM Journal of Numerical Analysis* 17 (1980) 883–893.
[16] R.D. Fierro, J.R. Bunch, Collinearity and total least squares, *SIAM Journal on Matrix Analysis and Applications* 15 (4) (1994) 1167–1181.
[17] E. Jacquelin, A. Bennani, P. Hamelin, Force reconstruction: analysis and regularization of a deconvolution problem, *Journal of Sound and Vibration* 265 (1) (2003) 81–107.